ACS APPLIED MATERIALS & INTERFACES

Research Article

www.acsami.org

Multifunctional Hydrogel Microparticles by Polymer-Assisted Photolithography

Bin Li,[†] Muhan He,[†] Lisa Ramirez,[†] Justin George,[†] and Jun Wang*[,†,‡]

[†]Department of Chemistry, University at Albany, State University of New York, Albany, New York 12222, United States

[‡]Cancer Research Center, University at Albany, State University of New York, Rensselaer, New York 12144, United States

Supporting Information

ABSTRACT: Although standard lithography has been the most common technique in micropatterning, ironically it has not been adopted to produce multifunctional hydrogel microparticles, which are highly useful for bioassays. We address this issue by developing a negative photoresist-like polymer system, which is basically comprised of polyethylene glycol (PEG) triacrylate as cross-linking units and long-chain polyvinylpyrrolidone (PVP) as the supporting scaffold. We leverage standard lithography to manufacture multilayer microparticles that are intrinsically hydrophilic, low-autofluorescent, and chemically reactive. The versatility of the microparticles is demonstrated to be color-encoded, pore-controllable, bioactive, and potentially used as a DNA bioassay.

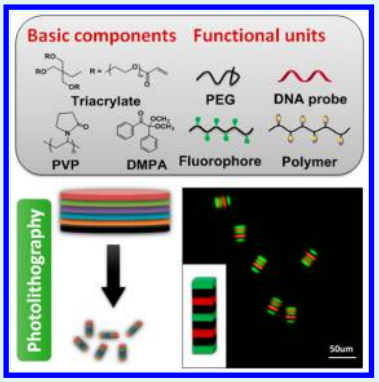

KEYWORDS: *photoresist, photolithography, multilayer, hydrogel, microarray*

1. INTRODUCTION

Photolithography based on photoresist and ultraviolet (UV) exposure has been the most fundamental technique in the microfabrication industry. Because standard photolithography permits fabrication of complex microstructures in a high-throughput fashion,[1,2] numerous photoresists and photoresist-like polymers have been introduced before. However, almost all of them are not amenable to biomolecule assays largely because of high autofluorescence.[3,4] On the other hand, hydrogel materials, such as peptides and functionalized polyethylene glycol (PEG), are naturally applicable to bioassays after micropatterning.[5−7] However, those materials are usually in aqueous solutions before photopolymerization, and therefore, the micropatterning cannot follow a standard photolithography process to develop complex microstructures. A few groups tried to mitigate that issue by developing new lithography approaches without fundamentally changing the composition of hydrogel materials. One approach is the stop-flow lithography and its derivatives, in which multi-streams of fluidic flow are converged and intermittently stopped for UV exposure to make barcoded microparticles.[8,9] The whole process is automated in a microfluidic chip, and millions of functional barcoded microparticles can be manufactured per hour. This microparticle production technology has shown certain utilities in biosensing of proteins, DNA, and mRNA.[10−12] Another recently developed, proprietary strategy to produce multifunctional particles is particle replication in non-wetting templates (PRINT).[13,14] The applications of the PRINT technique, however, have primarily focused on the nanomedicine field for large-scale production of nanoparticles to deliver drugs.

Because standard photolithography is still the most reliable, robust, and convenient technique to make complex microstructures, the alternative option would be the development of photoresist substitutes that are intrinsically hydrophilic and chemically reactive. Semi-interpenetrating polymer networks (semi-IPNs) have been a promising candidate for fabricating hydrophilic microfeatures. Semi-IPNs are unique "alloys" of polymers, in which at least one network is cross-linked in the presence of long-chain polymers.[15] The entanglement of networks with polymer chains conveys the whole system mechanical strength and new chemical and biological properties that one network alone does not possess. Hydrogel semi-IPNs produced by photopatterning have been introduced before for applications in tissue engineering.[16] The drawback of those formulations, just like single-component hydrogel materials, is the incompatibility with standard lithography and the inability to fabricate complex microstructures.

Here, we report a polyvinylpyrrolidone (PVP)/PEG semi-IPN as the first photoresist-like material that can be used in standard lithography to fabricate complex microparticles for bioassays. By incorporation of functional units, the facile technique is demonstrated by manufacturing multilayer anisotropic microparticles that are encoded, functional, and potentially applicable in multiplexed DNA detection. It shows particular intriguing features, including a simple standard photolithography process, a small particle size at <10 μm

Received: December 7, 2015
Accepted: January 28, 2016

DOI: 10.1021/acsami.5b11883
ACS Appl. Mater. Interfaces XXXX, XXX, XXX−XXX

with an aspect ratio of >4, and an easy release from a substrate in an aqueous solution without an obvious change of shape and dimension, the combination of which are not achievable by other materials and methods.

2. MATERIALS AND METHODS

2.1. Materials. Trimethylolpropane ethoxylate triacrylate (M_n = 428 g mol^{-1}, PEG_{428} triacrylate, Aldrich), polyvinylpyrrolidone (M_n = 360 000 g mol^{-1}, PVP, Sigma), 2,2-dimethoxy-2-phenylacetophenone (DMPA, TCI), fluorescein isothiocyanate-dextran (M_n = 500 000 g mol^{-1}, FITC-dextran, Sigma), tetramethylrhodamine isothiocyanate-dextran (M_n = 500 000 g mol^{-1}, TRITC-dextran, Sigma), poly(allylamine hydrochloride) (M_n = 17 500 g mol^{-1}, PAH, Aldrich), biotin-PEG-biotin (M_n = 3400 g mol^{-1}, PEG-biotin, Laysan Bio), mPEG-carboxymethyl (M_n = 5000 g mol^{-1}, mPEG-CM, Laysan Bio), Cy5-streptavidin (Thermo Fisher Scientific), 1-ethyl-3-(3-(dimethylamino)propyl)carbodiimide hydrochloride (EDC·HCl, Thermo Fisher Scientific), *N*-hydroxysulfosuccinimide (sulfo-NHS, Thermo Fisher Scientific), acrylate-modified ssDNA oligomers (Acrydite, Integrated DNA Technologies, IDT; D, 5′-/5Acryd/AAA AAA AAA AAA AAT GGT CGA GAT GTC AGA GTA-3′; E, 5′-/5Acryd/AAA AAA AAA AAA AAT GTG AAG TGG CAG TAT CTA-3′), Cy3-conjugated DNA (Integrated DNA Technologies, IDT; Cy3-D′, 5′-/5Cy3/AAA AAA AAA AAA ATA CTC TGA CAT CTC GAC CAT-3′; Cy3-E′, 5′-/5Cy3/AAA AAA AAA AAA ATA GAT ACT GCC ACT TCA CAT-3′), isopropyl alcohol (IPA, VWR), dimethylformamide (DMF, VMR), hydrogen peroxide (H_2O_2, VWR), and sulfuric acid (H_2SO_4, VWR) were used as received. Chrome photolithography masks were designed in-house using AutoCAD software and printed by Front Range PhotoMask Co. (Palmer Lake, CO)

Hydrogel microparticles were prepared by UV-initiated free radical polymerization of acrylate in the polymer matrix. A typical composition of the initial pre-polymer mixture consisted of 11.5 wt % PVP, 20.6 wt % PEG_{428} triacrylate, 2.8 wt % DMPA, and 65.1 wt % DMF.

2.2. Photolithographic Synthesis of Multilayer Microparticles. Typically, a uniform layer was first formed by spinning 1 mL of the pre-polymer mixture onto a silicon wafer at 1000 rpm for 30 s using a spin coater (WS-650MZ-23NPPB, Laurell). The wafer was then prebaked at 95 °C for 2 min to evaporate the organic solvent. After cooling to room temperature, the second layer was created on the solidified film by spin coating the pre-polymer mixture, as specified above. The multilayer film was stacked through repetitive spin coating and baking until the desired number of layers was reached. The solid multilayer film was then exposed to 320−500 nm light for 50 s at 120 mW cm^{-2}, irradiated from an UV lamp (OmniCure Serise 1000, Lumen Dynamics) through a chrome photomask with specific features. After exposure, the micropatterns were developed by immersing the silicon substrates in IPA to wash away the unpolymerized region. The microparticles were released by immersing the silicon wafer in TET buffer [1× Tris−EDTA (TE) with 0.05% (v/v) Tween-20], collected, and observed via an inverted optical microscope (IX73, Olympus) mounted with a digital camera (Zyla sCMOS, Andor).

2.3. Synthesis of Color-Encoded Multilayer Pallets. For the building of the color-coded multilayer, 6.7% (v/v) of 10 mg mL^{-1} FITC- or TRITC-dextran solution (1× TE at pH 8.0) was mixed with the pre-polymer solution and processed with the same protocol detailed above. The images of encoded particles were acquired directly using optical and fluorescence microscopies. Fluorescent micrographs were analyzed using ImageJ [National Institutes of Health (NIH)], and intensity was quantified along the axis of the particle for each fluorescence channel.

2.4. Synthesis and Characterization of Porosity-Tuned Hydrogel Microparticles. To enhance the accessibility to bioanalytes of large molecular weight, porosity was created by incorporation of PEG_{200} as porogen. Instead, the precursor solution was composed of 16.5 wt % PEG_{428} triacrylate and 4.1 wt % PEG_{200}, with the same ratio of PVP, DMPA, and DMF as mentioned above.

The diffusion of Cy3-DNA into hydrogel pallets was monitored with an inverted fluorescence microscope. First, 10 μL of microparticle suspension was added to 20 μL of TETB buffer (Tris−EDTA−Triton X-100 buffer with 500 mM NaCl). After a gentle vortex for 15 min, 10 μL of Cy3-DNA (0.5 μM, 1× TE at pH 8.0) was mixed with the microparticles and fluorescence images were captured at 5, 30, and 120 min of incubation. Relative fluorescence intensities were defined as the ratio of the average fluorescence intensity within the pallets to the average fluorescent signal in the bulk solution.

2.5. DNA Hybridization Assay. Acrydite-tagged oligo DNA was dissolved in deionized (DI) water at a stock concentration of 0.5 mM. A 10% (v/v) DNA oligomer solution was mixed with the pre-polymer mixture for the fabrication of the DNA detection layer. The DNA hybridization assay was accomplished by incubating the DNA-probe-embedded microparticles with target oligomer solution (0.5 μM, 1× TE) in TETB solution for 2 h with gentle shaking. The hybridized microparticles were washed with TET buffer before imaging. Fluorescent intensity was quantified along the axis of the particle using ImageJ.

2.6. Synthesis and Functionalization of Polymer-Incorporated Microparticles. *2.6.1. Construction of Two-Layer Microparticles with PAH.* A 14.3% (v/v) PAH solution (2.5%) was first mixed with the pre-polymer solution and fabricated as the second layer using the same protocol detailed above. The PAH particles were collected in distilled water and stored at 4 °C for further use.

PEG was conjugated via two-step coupling of mPEG-CM using EDC and sulfo-NHS. Briefly, 4 mg of EDC·HCl and 7 mg of sulfo-NHS were added to 150 μL of $mPEG_{5000}$-CM solution (15%, PBS6.0), and the mixture was stirred for 1 h at room temperature. The activated PEG solution was directly mixed with 1.2 mL of PAH particle dispersion (6×10^4 mL^{-1}, 0.1 M sodium bicarbonate buffer) and incubated for 3 h at room temperature with continuous stirring. The PEG-conjugated particles were finally purified by washing with PBS at pH 7.4 3 times and stored at 4 °C.

The absorption of Cy3-DNA onto the polymer-functionalized microparticles was performed as follows: 5 μL of Cy3-DNA (0.5 μM, 1× TE at pH 8.0) was mixed with 20 μL of microparticle suspension in PBST buffer [PBS7.4 with 0.05% (v/v) Tween-20] and gently vortexed for 1 h. The microparticles were washed with PBST buffer before imaging. Relative fluorescence intensity was defined as the average fluorescence intensity within the pallets minus the average fluorescent signal in the background acquired by ImageJ.

2.6.2. Construction of Two-Layer Microparticles with PEG-Biotin. A total of 3.3 wt % PEG-biotin was first dissolved in the pre-polymer solution and fabricated as the second layer using the same protocol detailed above. The fabricated particles were collected in distilled water and stored at 4 °C for further use.

Streptavidin tagging on one layer of a particle was achieved via streptavidin−biotin interactions. Typically, 5 μL of Cy5-streptavidin (50 μg mL^{-1}, PBS7.4) was mixed with 20 μL of microparticle suspension in PBSTP buffer [PBS7.4 with 0.05% (v/v) Tween-20 and 1 wt % bovine serum albumin] and gently vortexed for 1 h. The microparticles were washed with PBSTP buffer before imaging. Relative fluorescence intensity was defined as the average fluorescence intensity within the pallets minus the average fluorescent signal in the background acquired by ImageJ. Two-layer particles without PEG-biotin were also tested as the negative-control group.

3. RESULTS AND DISCUSSION

To optimize the photoresist composition, an array of hydrophilic polymers and monomers were first surveyed and eventually narrowed down to the PVP/PEG-triacrylate system, which gave the best fabrication results (detailed elucidation of the compositions and fabrication particularities was provided in the Supporting Information and Figures S1−S7). Briefly, PEG-triacrylate was selected as the cross-linkable monomer, which showed higher cross-link density after fabrication and resulted

DOI: 10.1021/acsami.5b11883
ACS Appl. Mater. Interfaces XXXX, XXX, XXX−XXX

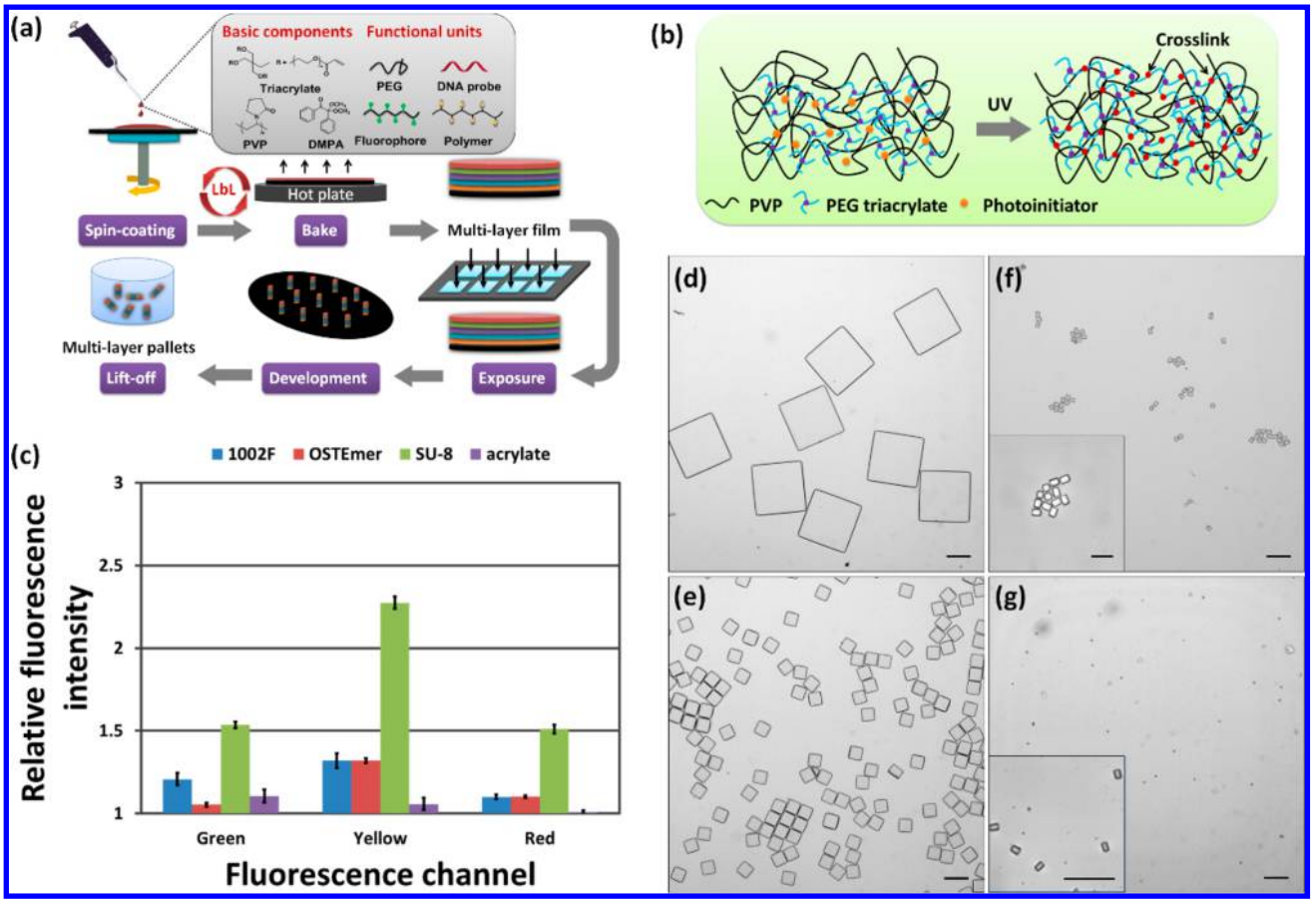

Figure 1. Fabrication of microsize patterns by standard lithography using PVP/PEG-triacrylate photoresist. (a) Schematic illustration of photolithography for synthesis of multilayer particles. (b) Cross-link mechanism of PEG-triacrylate in the PVP matrix to form a semi-interpenetrating network. Acrylate groups between PEG-triacrylate molecules react via radical photoinitiation to form a cross-linked polymer surrounding PVP. (c) Comparison of autofluorescence of micropatterns formulated by different photoresists. The relative fluorescence intensity is the normalized fluorescent intensity of the micropatterns to the background. Error bars are the standard deviation of the mean (n = 5). Micropatterns were fabricated using a chrome mask with 15 μm square patterns. Microscope images of lifted micropatterns with the size of (d) 200 μm, (e) 50 μm, (f) 15 μm, and (g) 5 μm. The insets of panels f and g show zoom-in images. Scale bar = 100 and 50 μm in the insets, respectively.

in a well-maintained shape and less swelling compared to PEG-diacrylate (Figure S1 of the Supporting Information). The PVP/PEG-triacrylate system was designed in a way that the high-molecular-weight PVP was taken as the scaffold for filling PEG-triacrylate, which was fluidic at an ambient environment. The high glass transition temperature (T_g > 150 °C[17]) of PVP facilitated the trapping of PEG-triacrylate inside of the mesh, and the whole system became solid without solvent, which was required before UV exposure or alignment in standard lithography. The compatibility of polymer, monomer, and solvent was critical for the success of designing such a semi-IPN. For example, poly(vinyl alcohol) (PVA) was found not compatible with PEG_{428}-triacrylate, and PEG_{428}-triacrylate showed poor solubility in water. The other consideration was that both PVP and PEG were hydrophilic, non-charged, and nontoxic, which would be the ideal case for future biomedical-related applications.

The basic PVP/PEG-triacrylate pre-polymer mixture includes $PVP_{360\,000}$, PEG_{428}-triacrylate, DMF as the solvent, and a photoinitiator DMPA. The fabrication process using this formulation is the same as conventional negative photoresists, while ours has a certain superiority in that it allowed for multilayer stacking before UV exposure and incorporation of various water-soluble functional units. As shown in Figure 1a, the pre-polymer mixture was first spin-coated on a silicon wafer, followed with a prebaking step. During that step, DMF contained in the mixture evaporated completely, resulting in a hardened, homogeneous layer on the wafer, where condensed long PVP chains were entangled as a physical network to prevent free diffusion of PEG-triacrylate. The prebaking temperature was set at 95 °C below the T_g of PVP to suppress the movement of polymer segments. After cooling to room temperature, another layer of pre-polymer could be coated on top of the prior layer through the same procedure. This repetitive coating−prebaking−cooling cycle permitted layer-by-layer (LbL) stacking of multiple layers without affecting downstream lithography. The solid multilayer film was then exposed to UV light through a patterned photomask, which induced the free-radical photopolymerization of triacrylate in the transparent region (Figure 1b), and intra- and interlayer cross-linking proceeded promptly as a result of the high reactivity of acrylate to radicals. After UV exposure, permanent interpenetrating PVP and PEG polymer networks were formed with double cross-links contributed by a branched structure of triacrylate and chemical binding. In the development step, the unexposed areas were dissolved in IPA and the UV cross-linked areas were left on the wafer.

DOI: 10.1021/acsami.5b11883
ACS Appl. Mater. Interfaces XXXX, XXX, XXX−XXX

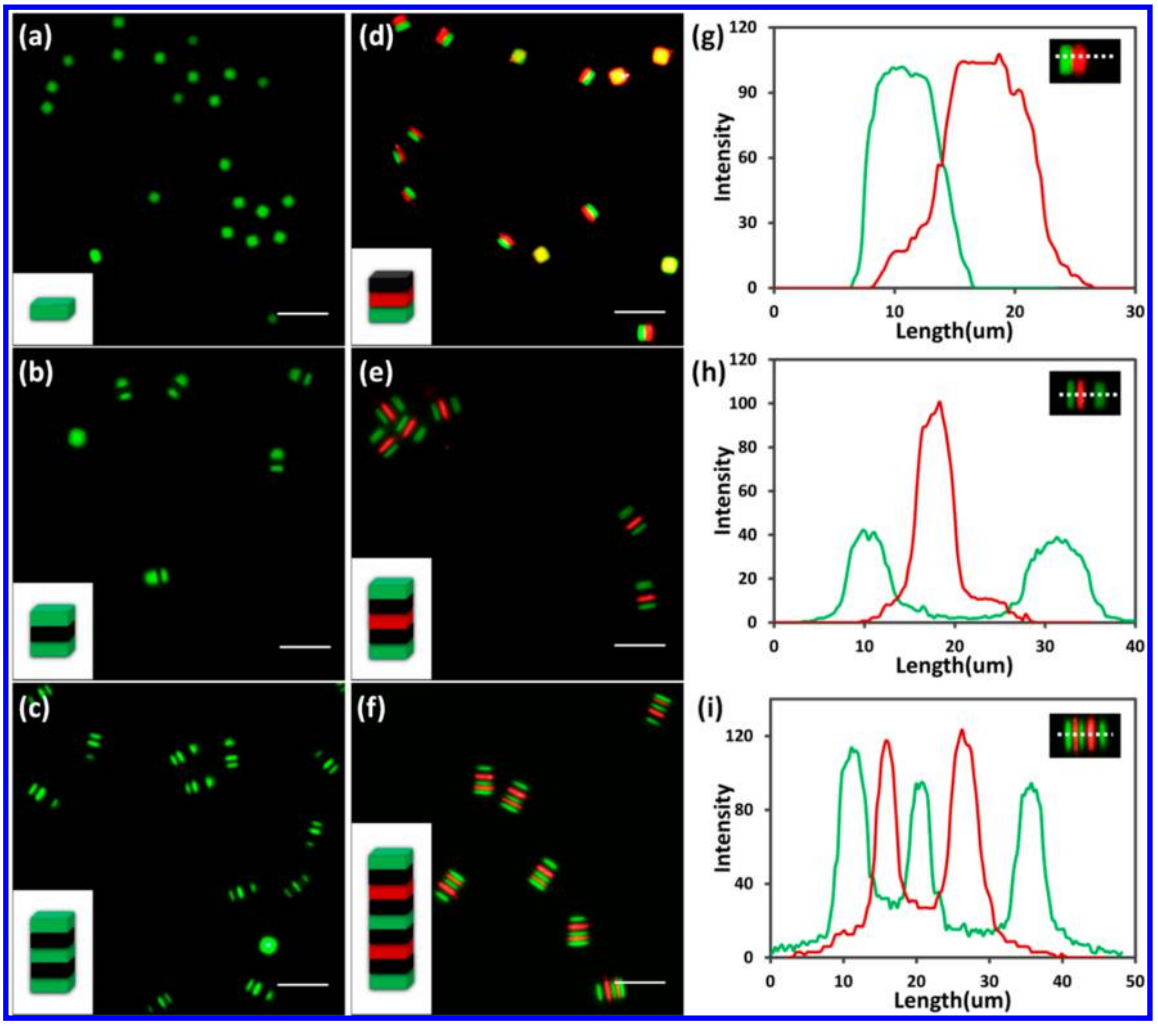

Figure 2. Color-coded multilayer particles fabricated by incorporation of FLPs. Fluorescent images of (a) one-layer, (b) three-layer, and (c) five-layer particles labeled with FITC-dextran (green). Fluorescent images of (d) three-layer, (e) five-layer, and (f) nine-layer particles labeled with FITC-dextran (green) and TRITC-dextran (red). The insets in panels a–f indicate the stacking formulation of multiple layers with FLP. Scale bars = 50 μm. (g–i) Fluorescent intensity plot of encoded particles in panels d–f along the axial line. Particles were fabricated using a mask with 15 μm square patterns.

Micropatterns can be easily lifted off from a wafer by simply immersing them in an aqueous solution. Monodispersed square microparticles of various sizes (5–200 μm) can be reliably fabricated and released by adjustment of the feature size of the mask (panels d–g of Figure 1). Moderate tunability of the PEG-triacrylate ratio from 37.5 to 64.2% (solid weight ratio) resulted in no loss of fabrication performance. The hydrogel-like microparticles were hydrated and swelled, dependent upon the percent of PEG-triacrylate in the semi-IPN (Figure S7 of the Supporting Information). Here, the micropatterns made by our method maintained the same shape in high fidelity; the swelling rate is typically <10%; and long-term storage did not cause the degradation or shape change of the hydrogel particles, indicative of a high cross-link density and stability of the network. Additionally, the autofluorescence of the micro-features made from PVP/PEG-triacrylate was negligible compared to commercial negative photoresists. As shown in Figure 1c, it exhibited the lowest fluorescence among SU-8 photoresist and other new photoresists, such as 1002F and OSTEmer.[3,4] The autofluorescence of PVP/PEG-triacrylate was $^1/_2$ of that of 1002F and 5 times lower than that of SU-8 photoresist in the green fluorescence channel, extremely low at the yellow fluorescence channel, and no autofluorescence at all in the red fluorescence channel. This property will be critical for any fluorescence-based bioassays.

The PVP/PEG-triacrylate system permits fabrication of multilayer microstructures and incorporation of compatible macromolecules in each layer. To demonstrate such a capability, we incorporated fluorophore-labeled dextran polymers (FLPs) with a weight ratio of 5.8‰ to PVP in the pre-polymer mixture, which was hypothesized to have minimal influence to the polymerization process and microparticle structures. FITC-dextran (excitation/emission: 492/518 nm) or TRITC-dextran (excitation/emission: 550/580 nm) was selectively mixed with the PVP/PEG-triacrylate pre-polymer before fabrication. Together with the blank layer without FLPs, color-coded multilayer particles could be fabricated with various codes. From the side view of fluorescent cylindrical particles (Figure 2 and brightfield images in Figure S8 of the Supporting Information), the sharp interface between different layers indicated the effective immobilization of FLP in the polymerized PVP/PEG semi-IPN. The pixel intensities (corresponding to the fluorescence intensities) were quantified along the axial line of each particle using ImageJ software.

DOI: 10.1021/acsami.5b11883
ACS Appl. Mater. Interfaces XXXX, XXX, XXX–XXX

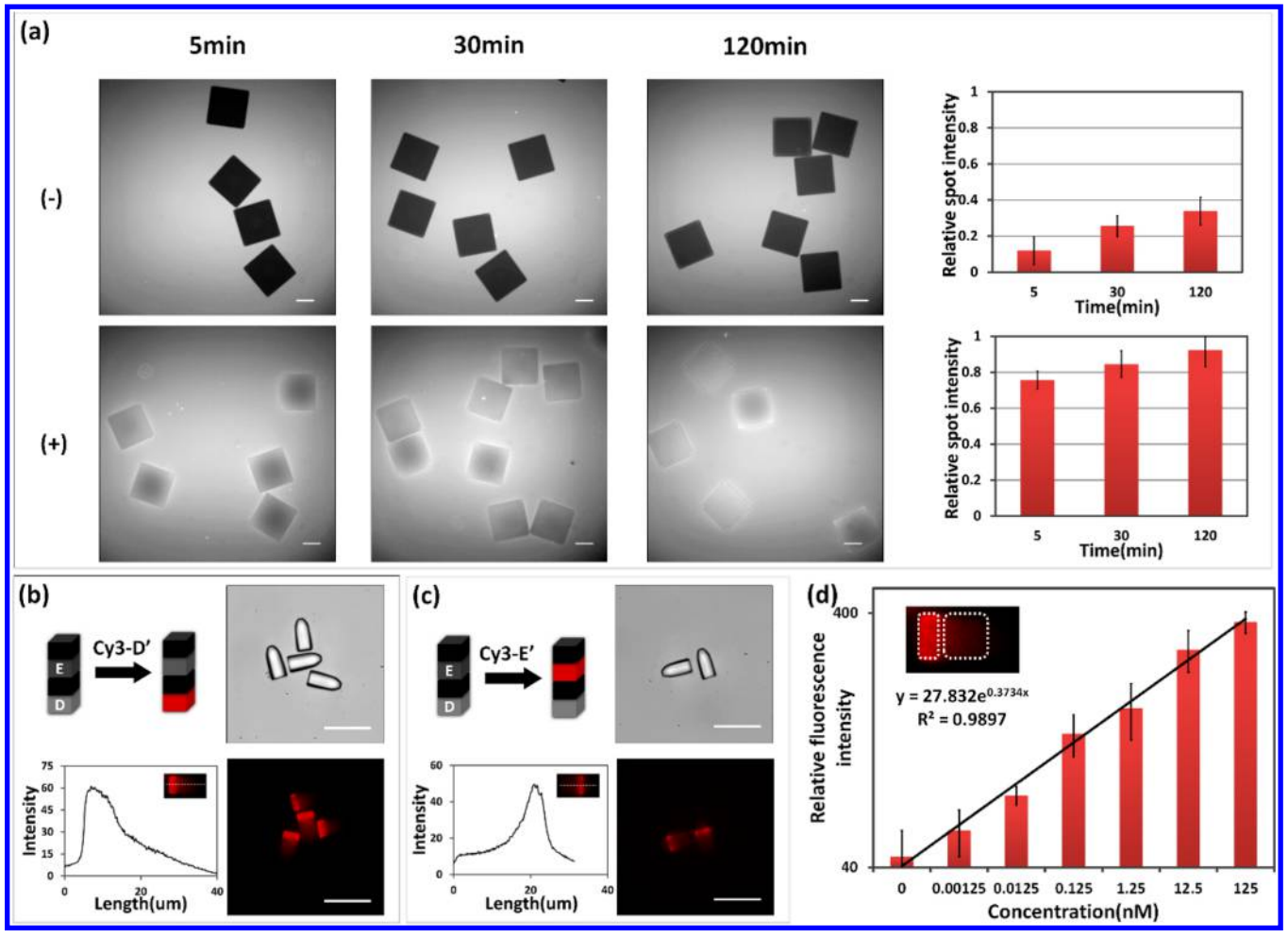

Figure 3. (a) Fluorescence images of Cy3-DNA diffusion into 200 μm hydrogel microparticles. The microparticles without PEG porogen (−, top) were formulated with 20.6 wt % PEG_{428}-triacrylate, while microparticles with PEG porogen (+, bottom) were composed of 16.5 wt % PEG_{428}-triacrylate and 4.1 wt % PEG_{200}. The relative fluorescence intensity in the right charts is the ratio of the average fluorescent intensity in the microparticles to the average intensity in the solution. (b and c) Multiplexed detection of Cy3-DNA oligomer using Acrydite-tagged oligo-DNA-incorporated four-layer particles of 15 μm size. The bottom profile is the fluorescence intensity along the axial line of a particle. Both brightfield and fluorescence images are shown on the right. (d) Detection of oligo DNA D′ at various concentrations. The relative fluorescence intensity denotes the quantitated fluorescence intensity of the detection region minus that of the region not for detection on the same particle (inset picture). Both concentration and relative fluorescence intensity are plotted on a log scale. The linear curve fit the data from 0 pM to 125 nM with R^2 = 0.9897. Error bars are the standard deviation of the mean (n = 5). Scale bars = 100 μm in panel a and 50 μm in panels b and c.

Panels g, h, and i in Figure 2 showed the fluorescence intensity profiles for three-, five-, and nine-layer microparticles (panels d–f of Figure 2), respectively. The separation of layers was fairly clear. There was a certain overlay between layers in the fluorescence profile, which might be caused by a slight overlap of emission spectra for FITC and TRITC. This clear separation rendered the possibility of encoding the microparticles by colors to produce barcode particles, as we have demonstrated here. For three codes, including green, red, and black, the nine-layer particles can theoretically have 19 683 (3^9) possibilities of combination that would be potentially applicable for a variety of high-throughput biological assays through generation of a library.[10,18−20]

The multilayer hydrogel particles that we fabricated can be highly porous for biomolecule diffusion by incorporation of pore generator (porogen). This feature has been leveraged to dramatically increase the surface/volume ratio for detecting multiple biomolecules on the same microparticle.[12,21] The 200 μm microparticles were first used to study the diffusion of biomolecules. As shown in Figure 3a and Figure S9 of the Supporting Information, the PVP/PEG particles were only slightly permeabilized by 33 nucleotide (nt) oligo DNA without adding porogen PEG_{200} in the pre-polymer mixture. With only 4.1 wt % PEG_{200} and slightly lower triacrylate cross-linking density, the microparticles were permeabilized by DNA within 5 min. PEG_{200}, as a small water-soluble molecule, was not covalently reacted with the polymer network, and it can be washed away after polymerization, leaving behind nanosize pores in the matrix.[12,22] Interestingly, the DNA permeation rate showed an opposite trend to the PEG molecular weight (Figures S10 and S11 of the Supporting Information), and the most significant enhancement of DNA diffusion was observed when PEG was lower than 1000, indicative that there may be a threshold for the pore generation efficiency of different PEG, while PEG bigger than 1000 was likely to be physically trapped inside the network.

Thus, the inner side of PVP/PEG semi-IPN becomes accessible using PEG_{200}, which will tremendously improve the sensitivity of DNA detection. We exemplified such a bioassay by incorporation of the DNA probe and detecting fluorophore

DOI: 10.1021/acsami.5b11883
ACS Appl. Mater. Interfaces XXXX, XXX, XXX−XXX

labeled 33 nt oligo DNA (Figure 3). Two oligo DNAs with acrylate group ending were anchored to the bottom layer and third layer of a four-layer microparticle during the fabrication step. They were used as the probes to detect their own complementary Cy3-labeled DNA (Cy3-DNA). As shown in panels b and c of Figure 3, the DNA oligomer targets were successfully hybridized with the proper layer in the particles without interference from other layers after incubation for 2 h. Calibration of DNA detection was investigated by varying the Cy3-DNA concentration. Figure 3d showed that the detection limit for 33 nt oligo DNA could be as low as 1 pM with a 10^5 linear range from ~1 pM to ~100 nM, and the fitted formula ($y = 27.832\ e^{0.3734x}$) was found to fit the data well, with $R^2 = 0.9897$. Given the high efficiency of incorporation of the DNA probe, the detection limit can be easily tuned depending upon the abundance of target DNA.

Last, we exhibit the flexibility of incorporating functional groups into the microparticles, which is usually lacking for most photoresists. First, PAH is selected with abundant amino groups, which is highly useful for bioconjugation. Using the same photolithography protocol, PAH was selectively inserted into the second layer of a two-layer microparticle at a weight ratio of 3.1% to PVP (Figure 4a). The accessible amino groups were confirmed by the DNA absorption test because DNA is negatively charged and PAH is positively charged at pH 7.4. As shown in panels b and c of Figure 4, Cy3-DNA was strongly absorbed on the exterior of the top layer, which was indicative of abundant amino groups left on the particle surface. The relatively low fluorescence inside the particles also implied the hindrance of DNA diffusion into the particles without porogen, which was consistent with the results shown in Figure 3. These amino groups were conveniently reacted with carboxylic PEG through carbodiimide cross-linker chemistry (Figure 4a). Therefore, the absorption of DNA was totally avoided after shielding the positive charges ($-NH_3^+$) of PAH and exhibited equal fluorescence intensity to the plain particles without incubation with Cy3-DNA (panels b and d of Figure 4).

Non-covalent interactions can also be introduced into our chemically anisotropic particles, which is exemplified by selectively anchoring streptavidin on one layer of a multilayer particle. The streptavidin–biotin interaction is widely used in bioassays because of a few advantages over other interactions.[23,24] Biotinylated PEG was dissolved in the pre-polymer solution and was retained in the second layer of a two-layer microparticle (Figure 4e). The incorporation of PEG-biotin was validated by incubation of the two-layer particles with Cy5-labeled streptavidin (Cy5-streptavidin). As shown in panels f and g of Figure 4, the top layer of each microparticle showed a much stronger fluorescent signal than the bottom layer and control particles, which did not contain PEG-biotin.

In conclusion, we have developed a PVP/PEG-triacrylate system as a tunable photoresist material to fabricate hydrophilic, ultralow autofluorescence and multifunctional microparticles using standard lithography. Other macromolecules and functional groups can be incorporated into the polymer system for encoding the multilayer particles and potentially other applications. We simply demonstrate the use of the multilayer particles for detection of oligo DNA with sensitivity at ~1 pM. This exemplified semi-interpenetrating polymer-based material bridges the conventional lithography and the hydrogel particle field and broadens the choices of hydrophilic photoresist in biological application.

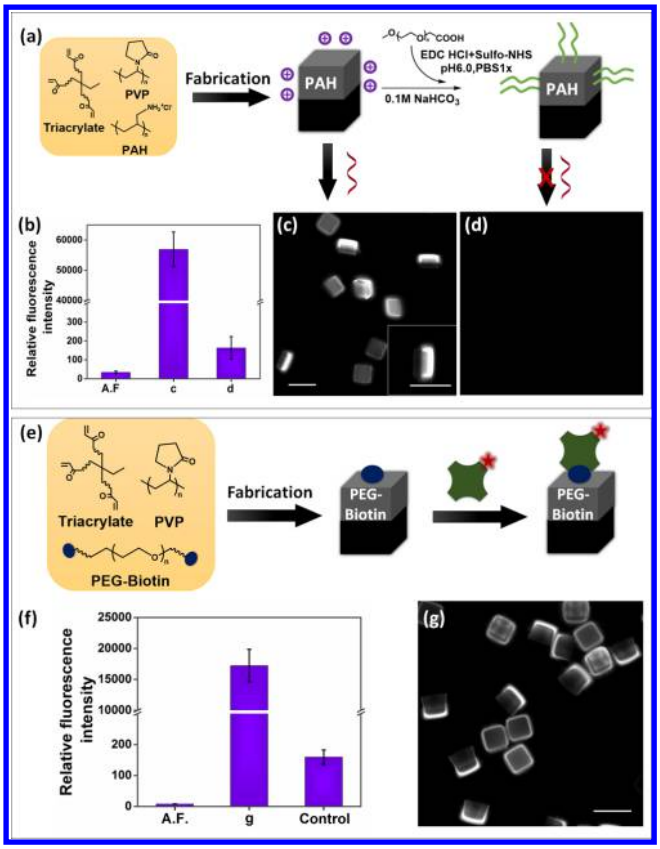

Figure 4. (a) Incorporation of chemically reactive groups to microparticles. (b) Relative fluorescence intensity of microparticles. The columns correspond to the relative fluorescence intensity of plain microparticles (A.F.), poly(allylamine hydrochloride) (PAH)-modified microparticles with Cy3-DNA absorption (bottom middle, c), and mPEG-carboxymethyl (mPEG-CM)-coated PAH microparticles with Cy3-DNA absorption (bottom right, d). (c) and (d) Fluorescence images of particles after incubation with Cy3-DNA. The inset in panel c shows a zoom-in image of one particle. Scale bar = 50 μm. (e) Incorporation of streptavidin–biotin interactions to microparticles. (f) Relative fluorescence intensity of microparticles. The columns correspond to the relative fluorescence intensity of plain microparticles (A.F.), PEG-biotin-modified microparticles after complex with Cy5-streptavidin (bottom right, g), and blank microparticles without PEG-biotin after incubation with Cy5-streptavidin (control). The relative fluorescence intensity is the average fluorescent intensity in the microparticles minus the average intensity in the background. (g) Fluorescence image of particles after incubation with Cy5-streptavidin. Scale bar = 50 μm.

■ ASSOCIATED CONTENT

Ⓢ Supporting Information

The Supporting Information is available free of charge on the ACS Publications website at DOI: 10.1021/acsami.5b11883.

Additional experimental results of fabrication and DNA diffusion (PDF)

■ AUTHOR INFORMATION

Corresponding Author

*E-mail: jwang34@albany.edu.

Funding

This work was supported by the Presidential Initiatives Fund for Research and Scholarship and startup fund by University at Albany, State University of New York to Jun Wang.

DOI: 10.1021/acsami.5b11883
ACS Appl. Mater. Interfaces XXXX, XXX, XXX–XXX

Notes

The authors declare no competing financial interest.

■ ACKNOWLEDGMENTS

The authors thank Dr. Jason Herschkowitz from the Cancer Research Center for helpful discussion and constructive advice.

■ REFERENCES

(1) Lin, Q. Properties of Photoresist Polymers. In *Physical Properties of Polymers Handbook*; Mark, J. E., Ed.; Springer: New York, 2007; Vol. *57*, pp 965−979, DOI: 10.1007/978-0-387-69002-5_57.
(2) Xia, Y.; Whitesides, G. M. Soft Lithography. *Annu. Rev. Mater. Sci.* **1998**, *28*, 153−184.
(3) Karlsson, J. M.; Carlborg, C. F.; Saharil, F.; Forsberg, F.; Niklaus, F.; Wijngaart, W.; Haraldsson, T. High-Resolution Micropatterning of Off-Stoichiometric Thiol-Enes (OSTE) via a Novel Lithography Mechanism. *Proceedings of the 16th International Conference on Miniaturized Systems for Chemistry and Life Sciences*; Okinawa, Japan, Oct 28−Nov 1, 2012; pp 225−227.
(4) Pai, J.-H.; Wang, Y.; Salazar, G. T. A.; Sims, C. E.; Bachman, M.; Li, G. P.; Allbritton, N. L. Photoresist with Low Fluorescence for Bioanalytical Applications. *Anal. Chem.* **2007**, *79*, 8774−8780.
(5) Hammoudi, T. M.; Lu, H.; Temenoff, J. S. Long-Term Spatially Defined Coculture Within Three-Dimensional Photopatterned Hydrogels. *Tissue Eng., Part C* **2010**, *16*, 1621−1628.
(6) Hahn, M. S.; Taite, L. J.; Moon, J. J.; Rowland, M. C.; Ruffino, K. A.; West, J. L. Photolithographic Patterning of Polyethylene Glycol Hydrogels. *Biomaterials* **2006**, *27*, 2519−2524.
(7) Meiring, J. E.; Schmid, M. J.; Grayson, S. M.; Rathsack, B. M.; Johnson, D. M.; Kirby, R.; Kannappan, R.; Manthiram, K.; Hsia, B.; Hogan, Z. L.; Ellington, A. D.; Pishko, M. V.; Willson, C. G. Hydrogel Biosensor Array Platform Indexed by Shape. *Chem. Mater.* **2004**, *16*, 5574−5580.
(8) Paulsen, K. S.; Di Carlo, D.; Chung, A. J. Optofluidic Fabrication for 3D-shaped Particles. *Nat. Commun.* **2015**, *6*, 6976.
(9) Dendukuri, D.; Gu, S. S.; Pregibon, D. C.; Hatton, T. A.; Doyle, P. S. Stop-flow Lithography in a Microfluidic Device. *Lab Chip* **2007**, *7*, 818−828.
(10) Pregibon, D. C.; Toner, M.; Doyle, P. S. Multifunctional Encoded Particles for High-Throughput Biomolecule Analysis. *Science* **2007**, *315*, 1393−1396.
(11) Appleyard, D. C.; Chapin, S. C.; Doyle, P. S. Multiplexed Protein Quantification with Barcoded Hydrogel Microparticles. *Anal. Chem.* **2011**, *83*, 193−199.
(12) Choi, N. W.; Kim, J.; Chapin, S. C.; Duong, T.; Donohue, E.; Pandey, P.; Broom, W.; Hill, W. A.; Doyle, P. S. Multiplexed Detection of mRNA Using Porosity-Tuned Hydrogel Microparticles. *Anal. Chem.* **2012**, *84*, 9370−9378.
(13) Wang, J. Y.; Wang, Y.; Sheiko, S. S.; Betts, D. E.; DeSimone, J. M. Tuning Multiphase Amphiphilic Rods to Direct Self-Assembly. *J. Am. Chem. Soc.* **2012**, *134*, 5801−5806.
(14) Zhang, H.; Nunes, J. K.; Gratton, S. E. A.; Herlihy, K. P.; Pohlhaus, P. D.; DeSimone, J. M. Fabrication of Multiphasic and Regio-specifically Functionalized PRINT ® Particles of Controlled Size and Shape. *New J. Phys.* **2009**, *11*, 075018.
(15) Myung, D.; Waters, D.; Wiseman, M.; Duhamel, P.-E.; Noolandi, J.; Ta, C. N.; Frank, C. W. Progress in the Development of Interpenetrating Polymer Network Hydrogels. *Polym. Adv. Technol.* **2008**, *19*, 647−657.
(16) Suri, S.; Schmidt, C. E. Photopatterned Collagen-hyaluronic Acid Interpenetrating Polymer Network Hydrogels. *Acta Biomater.* **2009**, *5*, 2385−2397.
(17) Buera, M. d. P.; Levi, G.; Karel, M. Glass Transition in Poly(vinylpyrrolidone): Effect of Molecular Weight and Diluents. *Biotechnol. Prog.* **1992**, *8*, 144−148.
(18) Kim, S.-H.; Shim, J. W.; Yang, S. M. Microfluidic Multicolor Encoding of Microspheres with Nanoscopic Surface Complexity for Multiplex Immunoassays. *Angew. Chem., Int. Ed.* **2011**, *50*, 1171−1174.
(19) Lee, H.; Kim, J.; Kim, H.; Kim, J.; Kwon, S. Colour-barcoded Magnetic Microparticles for Multiplexed Bioassays. *Nat. Mater.* **2010**, *9*, 745−749.
(20) Dejneka, M. J.; Streltsov, A.; Pal, S.; Frutos, A. G.; Powell, C. L.; Yost, K.; Yuen, P. K.; Müller, U.; Lahiri, J. Rare Earth-doped Glass Microbarcodes. *Proc. Natl. Acad. Sci. U. S. A.* **2003**, *100*, 389−393.
(21) Le Goff, G. C.; Srinivas, R. L.; Hill, W. A.; Doyle, P. S. Hydrogel Microparticles for Biosensing. *Eur. Polym. J.* **2015**, *72*, 386.
(22) Lee, A. G.; Arena, C. P.; Beebe, D. J.; Palecek, S. P. Development of Macroporous Poly(ethylene glycol) Hydrogel Arrays within Microfluidic Channels. *Biomacromolecules* **2010**, *11*, 3316−3324.
(23) Dundas, C.; Demonte, D.; Park, S. Streptavidin-biotin technology: Improvements and Innovations in Chemical and Biological Applications. *Appl. Microbiol. Biotechnol.* **2013**, *97*, 9343−9353.
(24) Cobo, I.; Li, M.; Sumerlin, B. S.; Perrier, S. Smart Hybrid Materials by Conjugation of Responsive Polymers to Biomacromolecules. *Nat. Mater.* **2015**, *14*, 143−159.

DOI: 10.1021/acsami.5b11883
ACS Appl. Mater. Interfaces XXXX, XXX, XXX−XXX